Colloidal particle aggregates induced by particle surface charge heterogeneity

S. Sennato [a,b], D. Truzzolillo [a,b], F. Bordi [a,b], F. Sciortino [a,b], C. Cametti [a,b,*]

[a] Dipartimento di Fisica, Universita' di Roma 'La Sapienza', Piazzale A. Moro 5, I-00185, Rome, Italy
[b] INFM CRS-SOFT, Unita' di Roma 1, Rome, Italy

ARTICLE INFO

ABSTRACT

Interaction of charged particles, induced by adding an oppositely charged polyion, gives rise to intriguing aggregation phenomena. The presence of short-range interactions in competition with electrostatic repulsions results, in an interval of concentrations around the inversion point, in the formations of long-lived clusters of polyelectrolyte-decorated particles. We will show that the whole aggregation scenario can be justified as due to an heterogeneous charge distribution at the particle surface, as a consequence of the correlated polyion adsorption, on the basis of a recently model proposed by D. Velegol, P. Thwar, Langmuir 17 (2001) 7687–7693.

© 2009 Elsevier B.V. All rights reserved.

1. Introduction

Recent experimental investigations have shown that charged colloidal particles form relatively large aggregates when interacting with oppositely charged polyions, these structures remaining stable in time for days or week [1–10]. Whether these aggregates represent a new true equilibrium phase or are they simply kinetically stabilized, is still matter of debate [11–13]. However, these aggregates represent a new class of colloids with fascinating and not yet completely understood properties and have a high potential for applications in biotechnology as bio-compatible vectors for intracellular multi-drug delivery. The formation of equilibrium clusters in different colloidal systems recently attracted vast interest [14]. The assembly is generally attributed to the interplay between competing interactions, a long-range electrostatic repulsion and some sort of short-ranged attractive force, depletion [15], for example, or forces due to a non-uniform distribution of the charge density at the particle surface [9]. As a consequence of the aggregation, a microphase separation into preferred aggregates of different size and shape occurs leading to the phenomenon of dynamical arrest mediated by clusters, and eventually to gelation processes [14]. Systems of charged colloids and oppositely charged linear polyelectrolyte represent, from this point of view, a particularly interesting class of long-range repulsive short-range attractive colloids, since, in this case, both repulsive and attractive interactions share a common electrostatic origin.

When the polyelectrolyte chains adsorb on the particle surface, due to the competing electrostatic interactions, that are attractive between the polymer and the oppositely charged surface and repulsive between the same charged polymers, a local ordering of the adsorbed chains results. This correlated distribution of the adsorbed chains is, in turn, the origin of a non-uniform distribution of the electric charge at the particle surface, which is now "decorated" by the adsorbed polyelectrolyte, showing alternate patches, where the polymer charge or that of the particle surface are locally in excess.

As it has been previously shown [16–18] between particles with such non-uniformly charged surfaces, an attractive interaction can arise also when the two particles bear net like charges.

The correlated adsorption is also the cause of the counterintuitive phenomenon of "overcharging", or charge inversion, which occurs when more polyelectrolyte adsorbs than is needed to neutralize the original charge of the surface so that the net charge of the polymer-decorated surface inverts its sign [19].

The driving force for the formation of the aggregates is mostly of electrostatic origin. Hence, being the repulsion due to the net like charges of the approaching particles and the attraction due to the charge non-uniformity, the aggregation process is expected to become more and more evident close the isoelectric point, where the net charge of the particles is almost zero and only the attractive part due to the charge non-uniformity survives. At that point, the colloid is expected to be completely destabilized. In fact, due to the concomitant overcharging effect, a peculiar phenomenology is observed. By adding increasing quantities of the polyion, with the progressive neutralization of the "decorated" particles, the size of the aggregates initially increases. At the isoelectric condition, when the overall charge of the polyion equals the overall charge

* Corresponding author. Fax: +30 06 4463158.
E-mail address: cesare.cametti@roma1.infn.it (C. Cametti).

at the particle surface, the size of the aggregates reaches its maximum value. However, beyond this point, their size decreases again, reaching the initial value that pertains to the isolated primary particles (or somewhat larger, due to an adsorbed polyelectrolyte layer) when the polyion is in large excess. This "re-entrant condensation" is probed by the average hydrodynamic radius of the aggregates, as measured by means of dynamic light scattering (DLS) techniques [3,20]. This behaviour can be justified considering that, beyond the isoelectric condition, the polyelectrolyte which is added in excess to the suspension, keeps adsorbing onto the particle surface, to an extent that depends in a complex way on the surface charge density, on the linear charge density of the polyelectrolyte and on its flexibility [19,21,22]. In this way, on the two sides of the isoelectric point, when the charge of the adsorbed polyions exceeds or falls short of the original charge of the particle by similar amounts, similar repulsions are experienced and the aggregates that form have similar sizes.

Recently, Nguyen and Shklovskii [23–25] explained both "charge inversion" and "re-entrant condensation" taking into account that, when the surface charge of the particle is reduced by condensed oppositely charged polyions, the correlation-induced short-range attraction dominates the long-range electrostatic repulsion, leading to the cluster formation.

Usually, by adding a simple electrolyte to a colloid, due to the increased screening of electrostatic repulsion, a process of aggregation is induced, with the formation of larger and larger aggregates that eventually ends with the separation of the solid phase (precipitation) [26]. On the basis of the classical Derjaguin–Landau–Verwey–Overbeek (DLVO) theory, one would expect that also the polyelectrolyte adsorption, partially neutralizing the particles, tends to destabilize the colloid, since the repulsion due to the ion diffuse layers overlap is reduced in proportion of the reduced net surface charge density [11,27].

In fact, close to the isoelectric point, in a narrow range of polyelectrolyte–particle concentration, such destabilization (and eventually the precipitation of the solid fraction) is actually observed [20]. However, in a wider concentration range, and almost symmetrically on both sides of the isoelectric point, the formation of long-lived, finite size aggregates overstays [28].

These aggregates have a size ranging from a few hundred nanometers (corresponding to a few primary particles stuck together) to a few microns, getting closer to the border of the "destabilization zone". They form almost immediately when the polyelectrolyte is added to the colloidal suspension and then remain stable in time for weeks, without showing any tendency toward further aggregation. The fast initial kinetics and the long-term stability, the reproducible increase of the aggregate size in getting closer and closer to the isoelectric point, the abrupt passage from a situation of stable aggregates to a destabilized colloid, all these facts rule out a simple phenomenon of "diffusional" kinetic stabilization.

A different mechanism must be invoked in order to justify the observed phenomenology. As we will show in the following, we will consider a mechanism based on a barrier potential that two approaching particles must overcome in order to stick together, with a height that increases with the size of the aggregates and depends on both the net charge and the non-uniform charge distribution on the primary particles.

This phenomenology has been observed in different polyelectrolyte–colloid systems, with solid particles (bare or lipid-coated polystyrene spheres [29]) or highly deformable, liquid filled lipid vesicles (liposomes) with the wall build up as a bilayer of different amphiphiles and with variable surface charge densities [3,4,20,28,30]. In what follow, we will focus on these vesicular systems that appear very interesting for their potential as bio-compatible vectors for intracellular multi-drug delivery. In fact, within the liposome clusters, as we have recently demonstrated [4,31] each vesicle maintains its individuality and its separate content. The aggregates, that can transport different drugs in the different compartments (liposomes), can be viewed as multi-compartment vectors, easy to assemble, with controlled size and net charge. Moreover, being the assembly based on physical mechanisms and not on a particular chemistry, the chemical composition of these vectors results very flexible and adaptable to different circumstances.

The purpose of this paper is to summarize some recent results obtained in our Laboratory dealing with the formation of complexes of liposomes built up by a cationic lipid, di-oleoyl-trimethyl-ammonium-propane (DOTAP), and a linear negatively charged polyion, poly(acrylate) sodium salt, that can be considered as a simple polyelectrolyte model. We will show that the whole phenomenology can be justified as due to a heterogeneous charge distribution at the particle surface, as a consequence of the correlated polyion adsorption. Adsorbed polyions are not positioned at random and correlation occurs because they reconfigure themselves in a short-range order, to gain some energy. The particle surface appears decorated by a more or less ordered "patchworm-like" pattern, with excess positive charge domains (polyion-free domains) and excess negative charge domains (polyion domains). From such a non-homogeneous surface charge distribution, a "short-range" attractive potential arises ("charge-patch" attraction) [32]. We will show that an appropriate interparticle potential built up by taking into account the heterogeneous charge distribution at the particle surface, such as the potential recently proposed by Velegol and Thwar [18], allows us to describe much of the phenomenology we observed in these systems, in particular the formation of large equilibrium aggregates. We refer here to DOTAP liposomes in the presence of anionic polyion poly(acrylate) sodium salt, but these findings have a more general validity extended to a broad variety of mesoscopic charged particles.

2. Experimental

2.1. Materials and liposome characterization

Positively charged liposomes were prepared by employing the cationic lipid di-oleoyl-trimethyl-ammonium-propane, purchased from Avanti Polar Lipids (Alabaster, AL) and used without further purification. The negatively charged polyelectrolyte sodium polyacrylate, $[-CH_2CH(CO_2Na)-]_n$ [Na-PA], with nominal molecular weight 60 kD, was purchased from Polysciences Inc. (Warrington, PA) as 25% aqueous solution. All liposomal samples and polyelectrolyte solutions were prepared in Milli-Q water, with electrical conductivity less than 1×10^{-6} mho/cm.

Liposomes were prepared by dissolution of an appropriate amount of DOTAP in methanol–chloroform solution (1:1, v/v). After overnight vacuum rotoevaporation of the solvent, the dried lipid film was re-hydrated with Milli-Q quality water. The re-hydration process was carried out for 1 h at a temperature of 40 °C, well above the main phase transition temperature of this lipid ($T_f \approx 0$ °C). In order to form small uni-lamellar vesicles, the lipid solution was sonicated for 1 h at a pulsed power mode, until the solution appeared optically transparent in white light. The solution was then filtered by means of a Millipore 0.4 μm polycarbonate filter.

Liposome size and size distribution were obtained from dynamic light scattering measurements. After sonication, liposomes have an average diameter of 80 ± 5 nm (intensity-averaged size distribution) with a moderate polydispersity of about 0.2, as expected for a rather homogeneous particle suspension. The pH of the suspensions was checked for each sample and was found to remain constant to about the value of pH 6.2.

2.2. Polyion-induced liposome aggregation

The formation of the polyion–liposome complex was promoted by adding 250 µl of polyion solution prepared at an appropriate concentration to an equal volume of liposome suspension, in a single mixing step, this mixing order being kept fixed in all the experiments. In each sample investigated, the lipid concentration was maintained constant to the value $C_L = 0.6$ mg/ml, for the Debye plot experiment, or $C_L = 0.8$ mg/ml according to the experimental set-up employed.

These concentration values correspond to a final liposome volume fraction of the order of 3×10^{-3}. The polyelectrolyte concentration was varied in an interval from 0.05 to 0.2 mg/ml, and the whole range of polyelectrolyte–liposome charge ratios in the vicinity of the isoelectric condition, where the re-entrant condensation occurs, was thoroughly explored.

Measurements of size and electrophoretic mobility of liposomes–polyelectrolyte complexes were performed at various temperatures, from 5 to 80 °C. Static light scattering measurements of the complexes were all performed at the temperature of 25 °C. The temperature was controlled within ±0.1 °C. Polyion–liposome complexes were formed immediately before each measurement by mixing equal volumes of the liposome suspension and polyion solutions at the appropriate concentration, as described elsewhere [4]. Before mixing, liposomes and polyelectrolyte solutions were thermostatted at the desired temperature.

The mixed sample was placed in a thermostatted cell for the measurement of both electrophoretic mobility and size and size distribution. Electrophoretic mobility measurements were performed 5 min after the mixing, immediately followed by size determination.

In the systems investigated, the presence of very large aggregates often makes light scattering-based experiments partially non-reproducible. Since large particles mainly scatter in the forward direction, the effects of these large aggregates can be greatly reduced by using backscattering detection technique. While this is only an advantage in dynamic light scattering, in static light scattering experiments, the use of a fixed angle backscattering geometry entails the disadvantage that the particle form factor cannot be obtained by using a Zimm plot [33]. Nevertheless, we chose a backscattering approach also for static light scattering experiment, to take advantage of using the same experimental set-up for simultaneous measurements, exactly on the same sample, of the dynamic (the average hydrodynamic radius of the particles) and static light scattering (the "apparent" molecular weight and the second virial coefficient), and of the electrophoretic mobility (the surface charge density of the aggregates, the ζ-potential), minimizing in this way possible spurious effects related to the time evolution of the samples.

2.3. Dynamic light scattering and electrophoretic mobility measurements

Both the size and size distribution and the electrophoretic mobility of the suspended particles were measured by means of an integrated apparatus, NanoZetaSizer (Malvern Instruments LTD, UK) equipped with a 5 mW He–Ne laser. In this way the size and the electrophoretic parameters of the particles can be measured on the same sample and almost simultaneously, reducing the experimental uncertainties related to sample preparation, thermal gradients and convective movement that, in the presence of large aggregates within the suspension, can be considerable.

Size and size distribution of liposomes and polyions–liposome aggregates were measured by means of dynamic light scattering technique, collecting the normalized intensity autocorrelation functions at an angle of 173° and analyzing the collected data by using the CONTIN algorithm [34], in order to obtain the decay time distribution of the electric field autocorrelation functions. Decay times are used to determine the distribution of the diffusion coefficients D of the particles, which in turn can be converted in a distribution of apparent hydrodynamic radii R_H using the Stokes–Einstein relationship $R_H = K_B T / 6\pi\eta D$, where $K_B T$ is the thermal energy and η the solvent viscosity. The values of the radii shown here correspond to the average values on several measurements and are obtained from intensity-weighted distributions.

The electrophoretic mobility measurements were carried out by means of the laser Doppler electrophoresis technique. The mobility u was converted into the ζ-potential using the Smoluchowski relation $\zeta = u\eta/\varepsilon$, where η and ε are the viscosity and the permittivity of the solvent phase, respectively.

2.4. Static light scattering measurements

In the framework of Rayleigh–Gans–Debye approximation [35], the scattered excess intensity due to a suspension of colloidal particles (considered monodisperse) can be written as:

$$\frac{KC_L}{R_\theta} = \frac{1}{M_w P(q\Delta r) + S(q\Delta R)V_s N_0 C_L} \tag{1}$$

where the Rayleigh ratio R_θ is defined as the light scattered at angle θ in excess of that scattered by the pure solvent divided by the scattered incident light and where C_L is the particle weight concentration, M_w the molecular weight, V_S the volume from which the scattered light is collected (scattering volume) and N_0 is the Avogadro number. The factor $P(q\Delta r)$ takes into account the effect of light interference within the same particle (Δr stands for the internal coordinates), and $S(q\Delta R)$ is the interparticle interference factor, ΔR being the center-of-mass coordinates. Finally, the optical constant K, for vertically polarized incident light, is defined as:

$$K = \frac{(2\pi^2)n^2}{\lambda^4 N_0}\left(\frac{dn}{dc}\right)^2 \tag{2}$$

with n and dn/dc representing the refractive index of the solvent and the refractive increment due to the suspended particles, respectively, and λ the wavelength of the light in vacuum. Under proper assumptions, Eq. (1) can be approximated as:

$$\frac{KC_L}{R_\theta} \simeq \frac{1}{M_w P(qd)} + 2A_2 C_L \tag{3}$$

which is commonly used to interpret the static light scattering spectrum (here d simply stands for a characteristic size of the particle). Eq. (3) allows us to obtain the weight-average molecular weight M_w of the scatterers and the second virial coefficient A_2 of the suspension. The second virial coefficient A_2 gives us a global information on the specific intermolecular interactions between the scatterers. It can be written (for a spherically symmetric interparticle potential) as:

$$A_2 = -\frac{N_0}{2M_w^2}\int_0^\infty (e^{-U_2/k_B T} - 1)4\pi r^2 dr \tag{4}$$

where U_2 is the two-particle potential energy [36]. A positive second virial coefficient (in homogeneous systems) means repulsive interactions. In order to cancel out the influence of M_w on A_2, it is convenient to express the second virial coefficient in dimensionless form as:

$$B_2 = A_2 \frac{M_w^2}{N_0 V} = -\frac{1}{2V}\int_0^\infty (e^{-U_2/k_B T} - 1)4\pi r^2 dr \tag{5}$$

where $V = 4\pi R^3/3$ is the volume of the aggregate, with R its average radius. In the presence of a "hard sphere potential", with interactions limited to the exclusion from the volume occupied by one

particle of other particles, $B_2 = 4$ [36]. Values higher than $B_2 = 4$ indicate stronger repulsions, while lower or negative values indicate attractive interactions between the particles in the suspension.

Unfortunately, in the present case, the form factor $P(qd)$ cannot be accurately determined and, consequently, the product $M_W P(qd)$ (the intercept of the Debye plots) cannot be separated into its factors. However, the quantity $M_W P(qd)$ can be considered as an effective molecular weight M_{weff} in calculating an "effective virial coefficient" $B_{2eff} = B_2 [P(qd)]^2$ (i.e., replacing M_W with $M_{weff} = M_W P(qd)$ in Eq. (5)). Since $P(qd)$ is ≤ 1 by definition, and it tends to the unity for small particles, a large increase of B_{2eff} over the value measured for the isolated liposomes, clearly indicates an increase of the repulsions, so that this quantity can be usefully employed to quantitatively characterize inter-aggregate interactions (Eq. (5)).

The evaluation of $P(qd)$ for polyion-decorated liposome aggregates is difficult to carry out, since such structures appear as compact clusters, but quite irregular and an analytical form of this factor does not exist, as is discussed elsewhere [9]. The impossibility of calculating the form factor from the geometry of the aggregates prevents the possibility of separating the effects due to the molecular weight M_W from those due the shape and size of the diffusing aggregate. Hence, in our analysis, the term $M_W P(qd)$ in Eq. (3), will be considered as an effective molecular weight M_{weff}.

3. Results and discussion

3.1. Electrostatic interactions

Both the typical effects observed in polyelectrolyte–oppositely charged colloid systems close to the isoelectric point, the "re-entrant condensation" and the "charge inversion" are illustrated in Fig. 1 in the case of two differently surface charged liposomes (cationic liposomes built up by cationic DOTAP and mixed liposomes built up by cationic DOTAP lipids and zwitterionic DOPE lipids). The complexation is carried out in the presence of varying amount of an anionic polyion, poly(acrylate) sodium salt [Na-PA]. As can be seen, at the isoelectric condition, where the overall charge of the aggregates passes through zero, the aggregates reach their maximum size. This condition is attained when the stoichiometric polyelectrolyte to lipid charge ratio ξ approaches the unity.

It must be noted, however, that this coincidence is accidental. In fact, on one hand, only the lipid molecules on the external leaflet of the bilayer (roughly one half of the total) have to be taken into account when the total charge on the liposomes is considered. On the other hand, because of the "counterion condensation" [37,38], the effective charge density of the polyelectrolyte may differ from its stoichiometric charge. In the present case, these two effects balance out almost exactly each other, although in other systems (for lipid coated polystyrene particles [29], for example) the isoelectric condition is attained for different values of the stoichiometric charge ratio.

In fact, when the linear charge density of the polyelectrolyte exceed a critical value, part of the counterions "condense" around the chain to reduce the density.

The critical value is usually assumed equal to e/l_B [37], with e the elementary charge and $l_B = \frac{e^2}{4\pi\varepsilon K_B T}$ the Bjerrum length. Within this picture, the fraction f of "free" (uncondensed) counterions is estimated to be of the order of $f = b/l_B$ (for both the counterions and the ionisable groups of the chain uni-valent), where b is the distance between the ionisable groups along the chain. For Na-PA the length b is ≈ 0.2 nm [39] and since in water and at room temperature (25 °C) the Bjerrum length is 0.71 nm, in these conditions the effective charge of Na-PA should reduce to ≈ 0.3 of its stoichiometric charge. This value which is in reasonable agreement with the
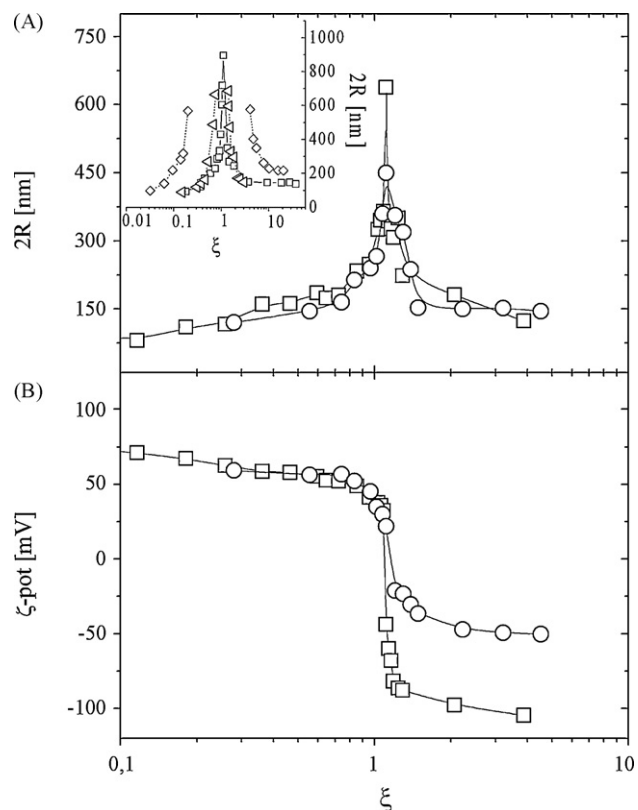

Fig. 1. Re-entrant condensation (aggregate size R, panel A) and charge inversion (ζ-potential, panel B) of positively charged liposomes in the presence of negatively charged Na-PAA polyions. Curves refer to different liposomal systems (□): DOTAP liposomes (2.87 mg/ml); (○): mixed DOTAP-DOPE liposomes (1:1 mol/mol) (0.84 mg/ml total lipid concentration). Inset in panel A shows the evolution of size for DOTAP liposomes and Na-PAA polyion aggregates in the presence of added NaCl salt: (△): 0.3 M; (◇): 0.4 M. Results obtained in the absence of salt (□) are also shown, for comparison.

one ($f = 0.35$) obtained for this polyelectrolyte, in aqueous solutions [40] and at the concentration employed here, from electrical conductivity measurements, might still appear a long way off from the figure of ≈ 0.5 which is needed to justify the position of the isoelectric point at $\xi \approx 1$ in Fig. 1. However, in the adsorption process the extent of the condensation can be modified by the electrostatic interaction with the oppositely charged surface [41], as we have shown in a recent paper [42].

The phenomenology is even more complicated, in the presence of an added simple salt such as, for example, NaCl salt. A typical result, as far as the re-entrant condensation is concerned, is shown in the inset of Fig. 1. Here, close to the isoelectric condition, a region of instability appears where the aggregates tend to flocculate rapidly, i.e., the solid phase separate and precipitate from the solution. This region widens as the salt concentration is increased. In the inset of Fig. 1, we show only the points corresponding to the stable aggregates, whose size increases getting closer and closer to the isoelectric point, the sudden stop of the curves marks the beginning of the instability region. The very narrow range of concentrations that marks the passage from the zone of finite size, stable aggregates to the instability condition is probably the sign that, by adding a simple salt, the phase diagram of the systems become more complex, with a new phase that appear at sufficient salt content, and that different mechanisms govern the formation of the stable aggregates and the continuous process of aggregation that eventually results in the flocculation.

As we already stated, the complex phenomenology we have briefly described above is common to a large variety of systems,

in particular cationic particles in the presence of anionic polyions [4,10,43,44] or, conversely, anionic particles in the presence of cationic polyions [6,7,45], giving further support to the relevance, for the aggregation process, of interactions of electrostatic origin.

3.2. Modelling the interactions

Due to the charge heterogeneity at the liposome surface as a consequence of the correlated polyion adsorption, the interparticle potential between two approaching spherical particles, according to the Velegol and Thwar model [18] can be written as:

$$\Phi_{AB}(H) = \frac{\varepsilon\pi R_A R_B}{R_A + R_B}\left[\left(\zeta_A{}^2 + \zeta_B{}^2 + \sigma_A{}^2 + \sigma_B{}^2\right)\ln\left(1 - e^{-2\kappa H}\right)\right.$$
$$\left. + 2\zeta_A\zeta_B\ln\left(\coth\left(\frac{\kappa H}{2}\right)\right)\right] \tag{6}$$

where R_A and R_B are the radii of the two interacting particles, ζ_A and ζ_B are the corresponding mean surface electrostatic potential assumed to be equal to the respective ζ-potential, ε is the dielectric permittivity of dispersing medium, $\kappa^{-1} = 4\pi l_B \sum_i c_i z_i^2$ is the Debye screening length (c_i is the number concentration of the z_i-valent ion) and H is the distance between the two particle surfaces measured along the segment connecting the centers of the two spheres (minimal distance between the surfaces).

In this model, the charge heterogeneity at the particle surface is taken into account through the variances σ_A and σ_B of the surface ζ-potential. Eq. (6), which is derived under the conditions $\kappa R_\alpha \ll 1$ and $H/R_\alpha \ll 1$ (α = A and B), holds under the following assumption: (i) ζ_A and ζ_B are relatively small (less than 25 mV at room temperature), (ii) the particles share the same chemical nature and are charged by similar mechanism and (iii) the Derjaguin approximation holds [46].

The Derjaguin approximation simply assumes that the surfaces of the interacting spherical particles can be described by a series of concentric flat rings. The approximation holds for $\kappa R_\alpha \ll 1$ and $H/R_\alpha \ll 1$. As a result, the generic force $F(h)$ between the surfaces of two spheres of radii R_A and R_B, at a distance h can be written [47] in terms of the potential $G(h)$ that would be observed were the two surfaces infinite planes at the same distance h as:

$$F(h) \propto \frac{R_A R_B}{R_A + R_B} G(h) \tag{7}$$

By the way, this expression clearly shows that, as a general rule and independently of the nature of the interparticle potential, whenever the Derjaguin approximation holds, the force between two spherical particles increases with their radius, toward the limiting force observed for two planes facing each other.

The potential described by the Eq. (6) depends on three parameters, i.e., the inverse of the Debye screening length κ, the average value of the surface potential (assumed in our calculations equal to the measured ζ-potential) and on the surface potential variance σ^2. In Fig. 2, we show the influence of these parameters on the reduced potential $\Phi/K_B T$ as a function of the minimal distance H. As can be seen, the height of the potential barrier increases with the increase of the ζ-potential and decreases with the variance. Conversely, the increase of the ionic strength (i.e., the decrease of the Debye length) influences only the range where the interaction occurs, not the barrier height.

However, as the ionic strength of the solution increases, the electrostatic interactions are more effectively screened and their range become comparable with the range of the dispersion forces (van der Waals term). In a more realistic model also these interactions
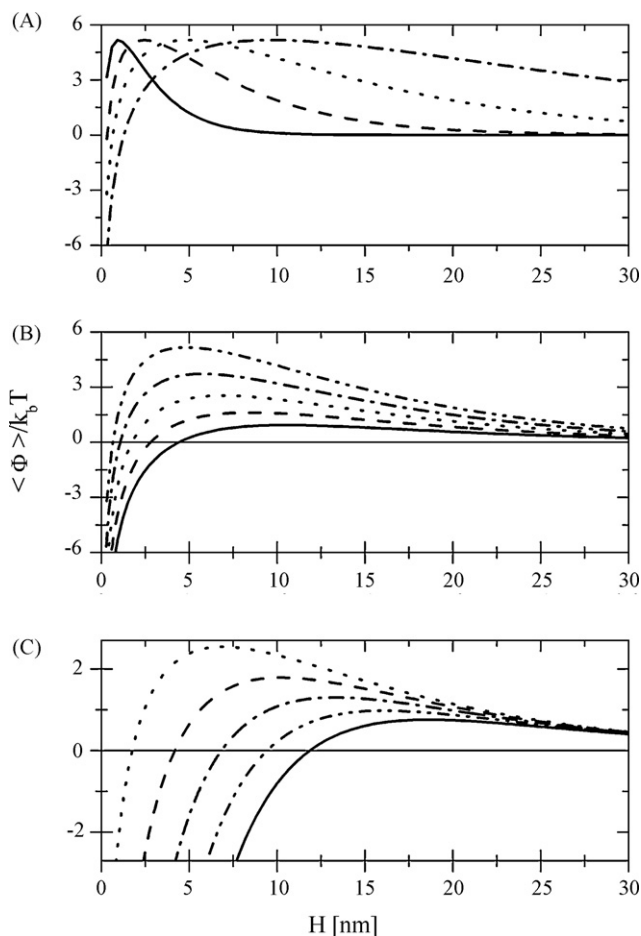

Fig. 2. Pair interaction potential curves according to Eq. (6) as a function of electrostatic parameters (κ, ζ-potential and variance σ^2) for $R_A = R_B = 40$ nm. Panel A: potential curves for $\zeta = 19$ mV, $\sigma = 15$ mV and for different values of κ: solid line, $\kappa = 0.05$ nm^{-1}; dashed line $\kappa = 0.1$ nm^{-1}; dotted line $\kappa = 0.2$ nm^{-1}; dash-dotted line $\kappa = 0.5$ nm^{-1}. Panel B: potential curves for $\kappa = 0.1$ nm^{-1} and $\sigma = 15$ mV and for different values of ζ-potential: solid line $\zeta = 11$ mV; dashed line $\zeta = 13$ mV; dotted line $\zeta = 15$ mV, dash-dotted line $\zeta = 15$ mV; dash-dotted line $\zeta = 19$ mV. Panel C: potential curves for $\zeta = 15$ mV, $\kappa = 0.1$ nm^{-1} and for different values of σ: solid line, $\sigma = 35$ mV; dashed line $\sigma = 30$ mV; dotted line $\sigma = 25$ mV; dash-dotted line $\sigma = 20$ mV; dash-dotted line $\sigma = 15$ mV.

must be taken into account. To this end a term [48]:

$$\Phi_{vdW}(H) = -A\frac{R_A R_B}{6(R_A + R_B)}\left(\frac{1}{H + h_A + h_B} - \frac{1}{H + h_A} - \frac{1}{H + h_B} + \frac{1}{H}\right)$$
$$- \frac{A}{6}\ln\left[\frac{H(H + h_A + h_B)}{(H + h_A)(H + h_B)}\right] \tag{8}$$

should be added to the potential (Eq. (6)). This expression, derived for shelled spheres with radius R_A and R_B and shell thickness h_A and h_B, respectively, appears appropriate for liposomes and liposome aggregates, where the presence of the water core substantially reduces the van der Waals attraction.

Fig. 3 shows the effect of the ionic strength on the "complete" potential of mean force $\Phi(H) = \Phi_{AB}(H) + \Phi_{vdW}(H)$. While the effect of the increasing ionic strength on the Velegol–Thwar potential is a simple translation on the logarithmic scale (dotted curves in Figs. 2 and 3, panel A)), the same parameter has a dramatic effect on the amplitude of the potential barrier when the dispersion forces are taken into the account, and above a certain salt content, the barrier completely vanishes and the colloid is totally destabilized. In Fig. 4, the potential of mean force $\Phi(H)$ is calculated for two different values of the particle radius (300 and 500 nm), at fixed
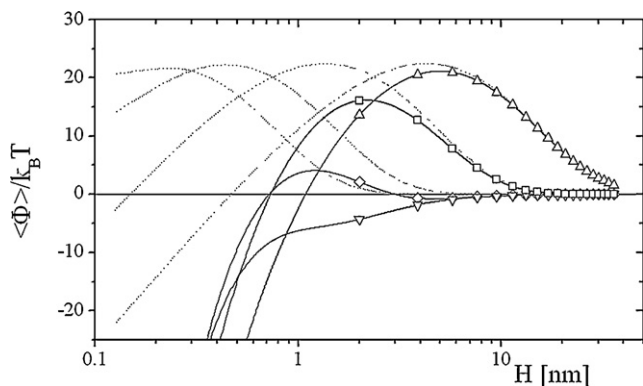
Fig. 3. The effect of the ionic strength on the complete pair interaction potential $\Phi(H) = \Phi_{AB}(H) + \Phi_{vdW}(H)$ (in units of the thermal energy at 25 °C). The curves are calculated for $R = 150$ nm, $\zeta = 20$ mV and $\sigma = 15$ mV, and for different values of the screening length κ^{-1}. ($\triangle$): $\kappa^{-1} = 9.6$ nm (corresponding to a 10^{-3} molar concentration of a symmetric univalent electrolyte), ($\square$): $\kappa^{-1} = 3.0$ nm (10^{-2} M), ($\lozenge$): $\kappa^{-1} = 0.96$ nm (10^{-1} M), ($\triangledown$): $\kappa^{-1} = 0.48$ nm (0.4 M). While the increasing ionic strength only translates the Velegol and Thwar potential (dotted curves) this parameter has a dramatic effect also on the amplitude of the potential barrier when the dispersion forces are taken in the due account. At moderate salt content, a secondary minimum appears and, as the ionic strength is further increased, the barrier vanishes and the colloid is completely destabilized.

ionic strength ($\kappa^{-1} = 3$ nm, corresponding to 10^{-2} M), and variance σ (15 mV), but for different values of the average surface potential ζ. It is clearly shown that there is a particular value of the ζ-potential (in this case ≈ 7.5 mV) that represents a sort of "threshold" for the instability. In fact above that value the potential barrier increases when the aggregate radius increases, so that, at any finite temperature, a given radius will be eventually "stabilized" when the potential barrier becomes exceedingly high in comparison with the thermal energy. However, below that "threshold" potential, since the barrier decreases with the aggregate radius, the aggregation process proceeds faster and faster to a complete destabilization of the colloid.

All these effects are completely consistent with the presence of an "instability region" (inset of Fig. 1) that is observed when a simple electrolyte is added to the solution. Unfortunately it is difficult to obtain an analytical expression of the potential barrier height for the potential $\Phi(H) = \Phi_{AB}(H) + \Phi_{vdW}(H)$, as a function of the aggregate radius. However, in the case of low ionic strength (no salt added
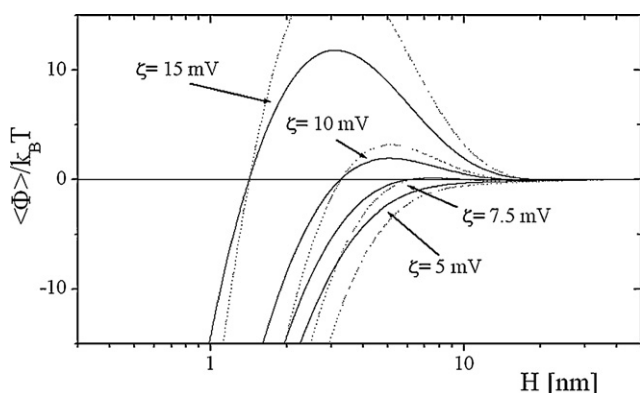

Fig. 4. The potential of mean force $\Phi(H) = \Phi_{AB}(H) + \Phi_{vdW}(H)$ between two identical spherical particles as a function of the minimum distance H between their surfaces. The potential is plotted in units of the thermal energy K_BT at room temperature (25 °C). The curves are calculated for $\kappa^{-1} = 3$ nm (10^{-2} M), $\sigma = 15$ mV, and for two different values of the radius $R = 300$ nm (full lines) and $R = 500$ nm (dotted lines), varying the average surface potential ζ. For a given ionic strength, a particular value of the potential ζ can be found that represents a threshold for the instability: above this particular value the potential barrier increases with the radius of the aggregate, below this value the barrier decreases.
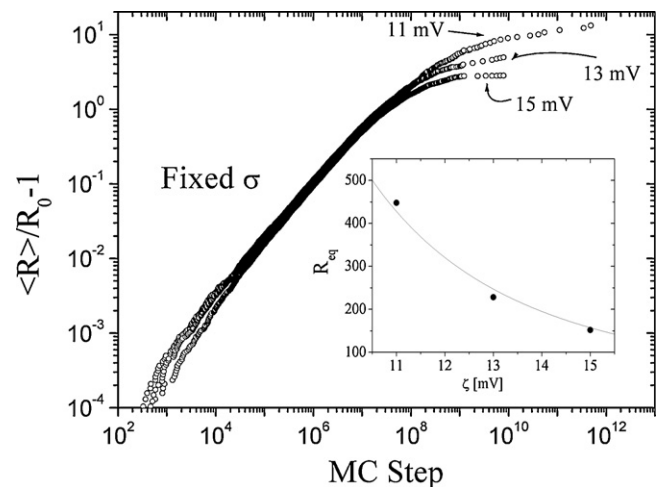

Fig. 5. MC step evolution of normalized mean cluster radius. Simulations have been carried out for different values of ζ-potential (11, 13 and 15 mV) with constant value of standard deviation $\sigma = 15$ mV and Debye constant $\kappa = 0.1$ nm^{-1}. Inset: mean normalized radius at the arrested states (filled black circles) compared with values obtained from Eq. (9).

and sufficiently low particle concentration), when the effect of the dispersion force can be ignored (see Fig. 3), the height of the potential barrier that two approaching particles must overcome in order to aggregate can be simply evaluated from Eq. (6). For two identical particles ($R_A = R_B = R$) we obtain:

$$
\begin{aligned}
\langle \Phi_{AB} \rangle_{max} = \varepsilon \pi R \Bigg\{ & \left(\zeta^2 + \sigma^2 \right) \ln \left[1 - \left(\frac{\zeta^2}{\zeta^2 + \sigma^2} \right)^2 \right] \\
& + \zeta^2 \ln \left[\frac{2\zeta^2 + \sigma^2}{\sigma^2} \right] \Bigg\}
\end{aligned}
\tag{9}
$$

In Fig. 5, we present MC-simulation results of the aggregation process investigated for different values of the ζ-potential, at a fixed value of the standard deviation σ. Our results show that, after a transient characterized by a rapid growth, almost independent of the values of the surface potential ζ, the system evolves toward a stationary state of finite aggregates whose size increases on decreasing the ζ-potential (i.e., getting closer to the isoelectric point). It is worth to note that, in all cases, the kinetic arrest occurs when the mean value of the potential barrier is of the order of 10 k_BT. In fact, if this value is considered in Eq. (9), a very good agreement is obtained with the average size of the aggregate at the kinetic arrest (see inset of Fig. 5).

3.3. The effect of temperature

Within the theoretical framework sketched above, the aggregation process in these systems can be described as an activated process. Briefly, a potential barrier arises from the combined effect of the screened electrostatic repulsion due to the overlap of the diffuse layers, and of the attraction, due to the non-uniform surface charge distribution (patch–charge attraction) arising from the correlated adsorption of the polyelectrolyte, and to the dispersion forces. At low ionic strength, when the electrostatic interactions are sufficiently long-ranged in comparison to the van der Waals forces, the potential barrier increases with the radius of the aggregates, so that at any finite temperature a limiting radius is stabilized. Conversely, as the electrostatic interactions are increasingly screened and their range become comparable with the range of the dispersion force, not only the potential barrier is lowered but its
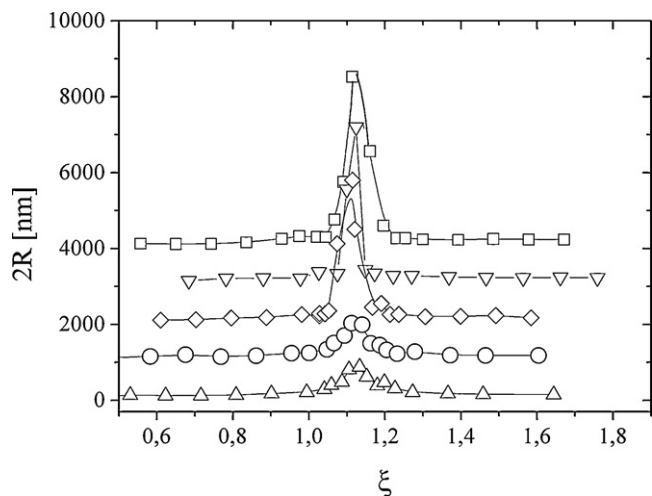
Fig. 6. Aggregate diameter of cationic DOTAP liposomes in the presence of anionic Na-PAA polyelectrolyte, for different temperatures investigated: ($\triangle$): 5 °C, ($\bigcirc$): 20 °C, ($\diamondsuit$): 40 °C, ($\triangledown$): 60 °C, ($\square$): 80 °C. Data are shown as a function of the polyion–lipid charge ratio parameter ξ. For clarity of presentation, values of size for curves at the different temperatures are shifted by addition of 1000 nm respect to the previous one.

height decreases with the increasing radius, so that the aggregates keep growing indefinitely and, in practice, a phase separation is observed. If this representation of the aggregation as a thermally activated process is correct, then the final cluster size should show an explicit dependence on temperature T, through the expression of the potential barrier height (Eq. (9)).

It could be interesting to determine if temperature changes really affect the cluster size, according to what is predicted by the explicit dependence on the temperature. To this point, answers the results plotted in Fig. 6, where we show the re-entrant condensation of the typical system formed by DOTAP liposomes and NaPAA polyions at different temperatures between 5 and 80 °C. The average size reached by the aggregates at their kinetic arrest is larger as the temperature is higher, providing typical evidence for a thermal activated process.

3.4. Interactions between the aggregates in the cluster phase

Within the "stability" region, the phase of long-lived cluster resulting from the fast aggregation process is characterized by the presence of strong repulsive interactions between the aggregates, whose strength increases with the size of the aggregates. This finding could be unexpected, since large stable aggregates mean low values of the surface potential ζ, and hence reduced electrostatic repulsions. However, to a more attentive view, it appears consistent with the characteristic of the potential $\Phi(H) = \Phi_{AB}(H) + \Phi_{vdW}(H)$ whose barrier increases with the particle radius.

We provide some experimental evidences of this increased repulsion for the larger aggregates that form in these colloid systems through the combined use of static and dynamic light scattering technique. Typical Debye plots of the light scattering data as a function of the liposome concentration C_L are shown in Fig. 7, for selected values of the polyelectrolyte–liposome molar ratio ξ, below, very close and above the point of charge inversion. Each sample, prepared at a fixed initial liposome concentration ($C_L = 0.6$ mg/ml), was progressively diluted and the excess Rayleigh ratio R_θ measured.

As can be seen in Fig. 7, panel A, with the increase of the polyion to lipid ratio ξ, and hence with the size of the aggregates, the slope of the curve $KC_L M_{weff}/R_\theta$ vs. C_L rapidly becomes steeper and steeper, reaches a maximum for samples which are very close to the charge
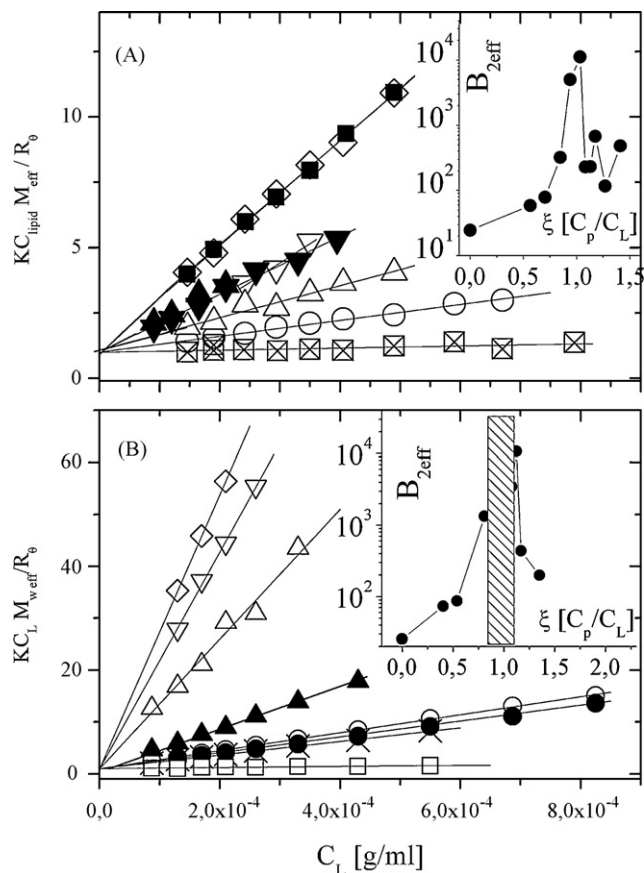

Fig. 7. Debye plot of polyion–liposome aggregates in absence of salt (panel A) and in the presence of 0.05 M NaCl (panel B). The ratio $KC_L M_{weff}/R_\theta$ is shown as a function of the liposome concentration C_L for different values of the polyelectrolyte–lipid molar ratio ξ, below (empty symbols) and above (open symbols) the isoelectric point. The constant behaviour for the liposomes without the added polyelectrolyte is also shown for comparison. Panel A: ($\boxtimes$): $\xi = 0$ (single liposomes), ($\bigcirc$): $\xi = 0.56$, ($\triangle$): $\xi = 0.70$, ($\triangledown$): $\xi = 0.85$, ($\diamondsuit$): $\xi = 0.99$, ($\blacksquare$): $\xi = 1.08$, (c): $\xi = 1.17$, and ($\blacktriangledown$): $\xi = 1.26$. Panel B: ($\square$): $\xi = 0$ (single liposomes), ($\times$): $\xi = 0.40$, ($\bigcirc$): $\xi = 0.54$, ($\triangle$): $\xi = 0.84$, ($\triangledown$): $\xi = 1.08$, ($\diamondsuit$): $\xi = 1.12$, ($\blacktriangle$): $\xi = 1.17$, and ($\blacklozenge$): $\xi = 1.35$. Insets show the second virial coefficient deduced from the respective Debye plots as a function of ξ. Shaded region in inset of panel B marks the polyion concentration region very close to the isoelectric point where DLS correlation function display two characteristic decay times.

inversion point and then decreases again towards the initial values (as the aggregates size decreases again).

A similar behaviour is shown in Fig. 7, panel B, where we show the slope of the curve $KC_L M_{weff}/R_\theta$ vs. C_L in the presence of added salt at a concentration of $C_S = 0.05$ mol/l. As we have already stated, in this region close to the isoelectric point, the suspension is not stable and often flocculates, with characteristic times that are not completely reproducible. For this reason, in our analysis, we did not consider samples inside this regions any further. However, outside this region, but sufficiently close to the isoelectric condition, the phenomenology described above in the absence of salt, i.e., an increase of repulsive interactions in vicinity of the isoelectric condition, is also observed in the presence of added salt.

Our results show that the second virial coefficient, which is related to the potential of mean force between two adjacent aggregates, markedly increases in the vicinity of the isoelectric point, i.e., where the aggregates are larger. We interpret this increase as a print of strong interparticle interactions and as a further support to the picture of a cluster phase stabilized, as sketched above, by a potential barrier.

Within this picture, also the apparently contradictory increase of the repulsive interactions observed when the ζ-potential goes to zero, can be justified. In fact, while close to the point of charge inver-
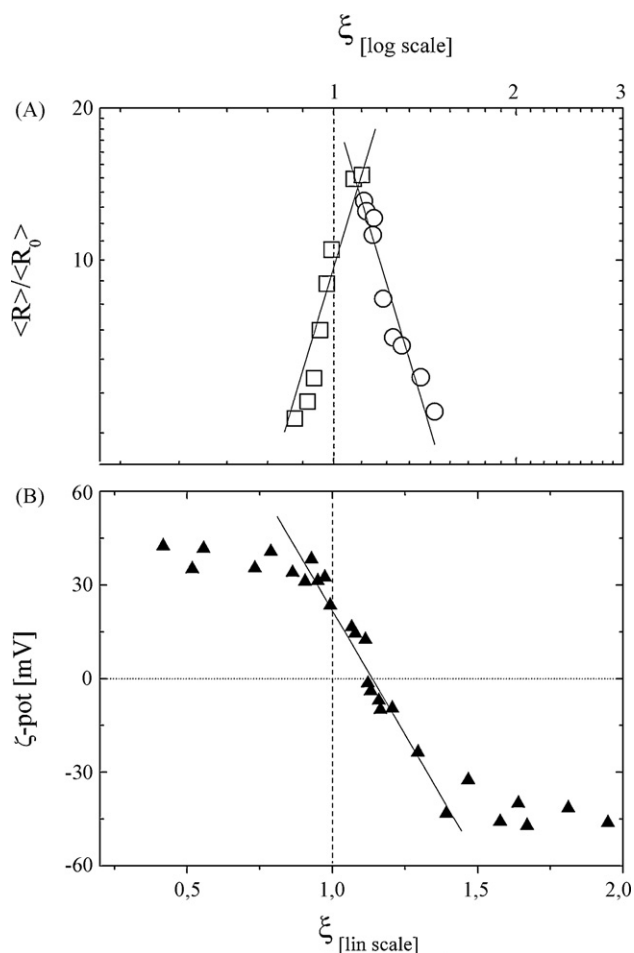
of the correlated polyion adsorption. The complex phenomenology these systems undergo, mainly the re-entrant condensation and the charge inversion, can be accounted for, at least to a first approximation, considering an interparticle potential recently proposed by Velegol and Thwar [18] which depends on two parameters, the ζ-potential and its variance σ^2 modified to take into account the short range ubiquitous van der Waals dispersion forces. This choice of the interparticle potential allows us to rationalize the complex experimental landscape shown by these systems describing, at least qualitatively, the observed phenomenology within a unified and consistent picture. Within this picture, the clusters would rather be kinetically stabilized than be true equilibrium aggregates, but with a mechanism which is completely different from the one usually assumed when destabilized, by reducing the screening length by increasing the ionic strength, the aggregates stop growing, and the flocculation process is apparently interrupted. In that case, the usual explanation is that the 'kinetic' stabilization is reached due to the progressive reduction of the mobility of the larger aggregates and to the low concentration that makes negligible the probability of a collision.

We have investigated the complexation of DOTAP liposomal particles in the presence of poly(acrylate) sodium salt below, close and above the isoelectric condition by means of dynamic light scattering and lased Doppler electrophoretic techniques and have studied the behaviour in the aggregation process by means MC simulation. These combined techniques offer a unifying scenario of the formation of a cluster phase that, for many of its characteristics, represent a new class of colloids. The overall above stated phenomenology is one, and for some aspects, new, of the facets of the complex formation in low-density colloidal suspensions.

Fig. 8. Behaviour of aggregate size (panel A) and ζ-potential (panel B) close to the isoelectric point. Superimposed lines shows the power laws fitting experimental data. Panel A: aggregate size grows as ξ^m, with $m = 4$; panel B: linear behaviour is found for ζ-potential. Note that log scale of panel A and linear scale of panel B are drawn to make the values $\xi = 1$ coincide.

sion, the ζ potential shows an approximately linear behaviour [9], the aggregate size diverges much more rapidly than linearly [9]. This means that the increase of the aggregate size over-compensates the decrease of the ζ-potential. Consequently, the height of the potential barrier maintains a finite value even if the overall charge of the aggregate tends to zero (ζ-potential tends to zero close to the point of charge inversion). Fig. 8 (upper part) shows, in a log–log scale, the divergent behaviour of the aggregate size close to the point of charge inversion. This behaviour is well approximated with a power law with an exponent of the order of 4.9. In the same figure (lower part), the approximately linear behaviour of the ζ-potential close to the charge inversion is also shown. For the example shown in Fig. 8, the increase of the barrier height as $\xi \to \xi_0$ is approximately evaluated as proportional to $R\zeta^2 \propto (\xi - \xi_0)^{-2}$. This finding supports the experimental results shown in Fig. 7, where we report an increase of the second virial coefficient close to the charge inversion condition.

4. Conclusions

In this note, we have summarized some recent experimental results from our laboratory providing evidence for the formation of relatively large, equilibrium clusters formed by charged colloidal particles stuck together by interactions with oppositely charged polyions. We have emphasized the role played by the heterogeneous charge distribution at the particle surface as a consequence

References

[1] E. Raspaud, I. Chaperon, A. Leforestier, F. Livolant, Biophys. J. 77 (1999) 1547–1555.
[2] Y. Wang, K. Kimura, P.L. Dubin, W. Jaeger, Macromolecules 33 (2000) 3324–3331.
[3] F. Bordi, C. Cametti, M. Diociaiuti, D. Gaudino, T. Gili, S. Sennato, Langmuir 20 (2004) 5214–5222.
[4] F. Bordi, C. Cametti, S. Sennato, M. Diociaiuti, Biophys. J. 91 (2006) 1513–1520.
[5] A.T.S. Yaroslavov, A. Rakhnyanskaya, Y. Ermakov, T. Burova, V.Y. Grinberg, F.M. Menger, Langmuir 23 (2007) 7539–7544.
[6] A.V. Sybachin, A.A. Efimova, E.A. Litmanovich, F.M. Menger, A. Yaroslavov, Langmuir 23 (2007) 10034–10039.
[7] D. Volodkin, V. Ball, P. Schaaf, J. Voegel, H. Mohwald, Biochim. Biophys. Acta 1768 (2007) 280290.
[8] E.V. Pozharski, R.C. MacDonald, Mol. Pharm. 4 (2007) 962–974.
[9] F. Bordi, C. Cametti, S. Sennato, D. Truzzolillo, Phys. Rev. E 76 (2007) 061403–61412.
[10] G. Gillies, W. Lin, M. Borkovec, J. Phys. Chem. B 111 (2007) 8626–8633.
[11] E. Pefferkorn, Adv. Colloids Interface Sci. 56 (1995) 33–104.
[12] F. Bordi, C. Cametti, M. Diociaiuti, S. Sennato, Phys. Rev. E 71 (2005) 050401(R)–050404(R).
[13] D. Truzzolillo, F. Bordi, F. Sciortino, C. Cametti, arXiv cond-matt:0804.0781 (2008).
[14] F. Sciortino, P. Tartaglia, Adv. Phys. (2005) 471–524.
[15] Y. Liang, N. Hilal, P. Langston, V. Starov, Adv. Colloid Interface Sci. 134–135 (2007) 151–166.
[16] S.J. Miklavic, D.Y.C. Chan, L.R. White, T.W. Healy, J. Phys. Chem. 98 (1994) 9022–9032.
[17] A.V.M. Khachatourian, A.O. Wistrom, J. Phys. Chem. B 102 (1998) 2483–2493.
[18] D. Velegol, P. Thwar, Langmuir 17 (2001) 7687–7693.
[19] A.Y. Grosberg, B.I. Shklovskii, T.T. Nguyen, Rev. Modern Phys. 74 (2002) 329–345.
[20] F. Bordi, C. Cametti, M. Diociaiuti, S. Sennato, Phys. Rev. E 71 (2005) 050401(R).
[21] T.T. Nguyen, A. Grosberg, B.I. Shklovskii, Phys. Rev. Lett. 85 (2000) 1568–1571.
[22] A.V. Dobrynin, A. Deshkovski, M. Rubinstein, Phys. Rev. Lett. 84 (2000) 3101–3104.
[23] T.T. Nguyen, B.I. Shklovskii, J. Chem. Phys. 114 (2001) 5905–5916.
[24] T.T. Nguyen, B.I. Shklovskii, J. Chem. Phys. 115 (2001) 7298–7308.
[25] T.T. Nguyen, B.I. Shklovskii, Rev. Mod. Phys. 74 (2002) 329–345.
[26] W.B. Russel, D.A. Saville, W.R. Schowalter, Colloidal Dispersions, Cambridge University Press, Cambridge, 1989.
[27] M. Borkovec, G. Papastavrou, Curr. Opin. Colloid Interface Sci. 13 (2008) 429–437.
[28] S. Sennato, F. Bordi, C. Cametti, J. Chem. Phys. 121 (2004) 4936–4940.
[29] S. Zuzzi, C. Cametti, G. Onori, Langmuir 24 (2008) 6044–6049.

[30] F. Bordi, C. Cametti, T. Gili, D. Gaudino, S. Sennato, Bioelectrochemistry 59 (2003) 99–106.
[31] F. Bordi, C. Cametti, S. Sennato, D. Viscomi, J. Colloids Interface Sci. 304 (2006) 512–517.
[32] S. Sennato, F. Bordi, C. Cametti, M. Diociaiuti, P. Malaspina, Biochim. Biophys. Acta 11–24 (2005) 1714.
[33] B.J. Berne, R. Pecora, Dynamic Light Scattering, Dover, New York, 2000.
[34] S. Provencher, Comput. Phys. Commun. 27 (1982) 213–227.
[35] J.K.G. Dhont, An introduction to dynamics of colloids, in: Studies in Interface Science, Elsevier, Amsterdam, 1996.
[36] D.A. McQuarrie, Statistical Mechanics, University Science Books, Sausalito, CA, 2000.
[37] G.S. Manning, Q. Rev. Biophys. 11 (1978) 179–246.
[38] A.V. Dobrynin, M. Rubinstein, Prog. Polym. Sci. 30 (2005) 10491118.

[39] K.S. Schmitz, J.-W. Yu, Macromolecules 21 (1988) 484–493.
[40] F. Bordi, R.H. Colby, C. Cametti, L. De Lorenzo, T. Gili, J. Phys. Chem. B 106 (2002) 6887–6893.
[41] T.T. Nguyen, A.Y. Grosberg, B.I. Shklovskii, J. Chem. Phys. 113 (2001) 1110–1117.
[42] F. Bordi, C. Cametti, S. Sennato, D. Viscomi, Phys. Rev. E 74 (2006), 030402–R.
[43] L. Ciani, S. Ristori, A. Salvati, L. Calamai, G. Martini, Biochim. Biophys. Acta 1664 (2004) 70–78.
[44] K. Keren, Y. Soen, G. Ben Yoseph, R. Yechiel, E. Braun, U. Sivan, Y. Talmon, Phys. Rev. Lett. 89 (2002) 88103–88106.
[45] S. Sennato, F. Bordi, C. Cametti, C. Marianecci, M. Carafa, M. Cametti, J. Phys. Chem. B 112 (2008) 3720–3727.
[46] R. Hogg, T.W. Healy, D.W. Fuerstenau, Trans. Faraday Soc. 62 (1966) 1638–1651.
[47] B. Todd, S.J. Eppell, Langmuir 20 (2004) 4892–4897.
[48] R. Tadmor, J. Phys.: Condens. Matter 13 (2001) L195–L202.